

# Harringtonine has the effects of double blocking SARS-CoV-2 membrane fusion

Shiling Hu<sup>1#</sup>, Nan Wang<sup>1#</sup>, Shaohong Chen<sup>2,3#</sup>, Qiang Ding<sup>4#</sup>, Cheng Wang<sup>1</sup>, Weina Ma<sup>1</sup>, Xinghai Zhang<sup>2</sup>, Yan Wu<sup>2</sup>, Yanni Lv<sup>1</sup>, Zhuoyin Xue<sup>1</sup>, Haoyun Bai<sup>1</sup>, Shuai Ge<sup>1</sup>, Huaizhen He<sup>1</sup>, Wen Lu<sup>1</sup>, Tao Zhang<sup>1</sup>, Yuanyuan Ding<sup>1</sup>, Rui Liu<sup>1</sup>, Shengli Han<sup>1</sup>, Yingzhan Zhan<sup>1</sup>, Guanqun Zhan<sup>1</sup>, Zengjun Guo<sup>1</sup>, Yongjing Zhang<sup>1</sup>, Jiayu Lu<sup>1</sup>, Jiapan Gao<sup>1</sup>, Qianqian Jia<sup>1</sup>, Yuejin Wang<sup>1</sup>, Hongliang Wang<sup>5</sup>, Shemin Lu<sup>6</sup>, Huajun Zhang<sup>2\*#</sup>, Langchong He<sup>1\*#</sup>

<sup>1</sup> School of Pharmacy, Xi'an Jiaotong University, Xi'an, China.

<sup>2</sup> State Key Laboratory of Virology, Wuhan Institute of Virology, Center for Biosafety Mega-Science, Chinese Academy of Sciences, Wuhan, China.

<sup>3</sup> University of Chinese Academy of Sciences, Beijing, China.

<sup>4</sup> School of Medicine, Tsinghua University, Beijing, China.

<sup>5</sup> Department of pathogen biology and immunology, School of Basic Medical Sciences, Xi'an Jiaotong University Health Science Center, Xi'an, China

<sup>6</sup> School of Basic Medical Sciences, Xi'an Jiaotong University, Xi'an, China.

#These authors contributed equally to this work.

\*Correspondence Author: Langchong He and Huajun Zhang

E-mail: helc@mail.xjtu.edu.cn, hjzhang@wh.iov.cn

## Address for correspondence

School of Pharmacy, Xi'an Jiaotong University, Yanta Westroad, Xi'an 710061, China.

State Key Laboratory of Virology, Wuhan Institute of Virology, Center for Biosafety Mega-Science, Chinese Academy of Sciences, Wuhan 430071, China

## **Abstract**

Fusion with host cell membrane is the main mechanism of infection of SARS-CoV-2. Here, we propose a new strategy to double block SARS-CoV-2 membrane fusion by using Harringtonine (HT), a small-molecule antagonist. By using cell membrane chromatography (CMC), we found that HT specifically targeted the SARS-CoV-2 S protein and host cell TMPRSS2, and then confirmed that HT can inhibit pseudotyped virus membrane fusion. Furthermore, HT successfully blocked SARS-CoV-2 infection, especially in the delta and Omicron mutant. Since HT is a small-molecule antagonist, it is minimally affected by the continuous variation of SARS-CoV-2. Our findings show that HT is a potential small-molecule antagonist with a new mechanism of action against SARS-CoV-2 infection, and thus HT mainly targets the S protein, and thus, greatly reduces the damage of the S protein's autotoxicity to the organ system, has promising advantages in the clinical treatment of COVID-19.

## Results and discussion

Since the outbreak of SARS-CoV-2 infection in December 2019, it has still wreaked havoc worldwide (**Fig. 1a, b**). Currently, many types of vaccines have been widely used for the prevention of SARS-CoV-2 infection<sup>1</sup>, while only two anti-COVID-19 drugs have been approved in the world<sup>2,3</sup>. These drugs target the replication process after SARS-CoV-2 enters host cells<sup>4,5</sup>. Given the continuous variation of SARS-CoV-2 into mutants such as Delta and Omicron mutants, effective therapeutic drugs that are capable to treat mutant infections are an urgent demand in the clinic.

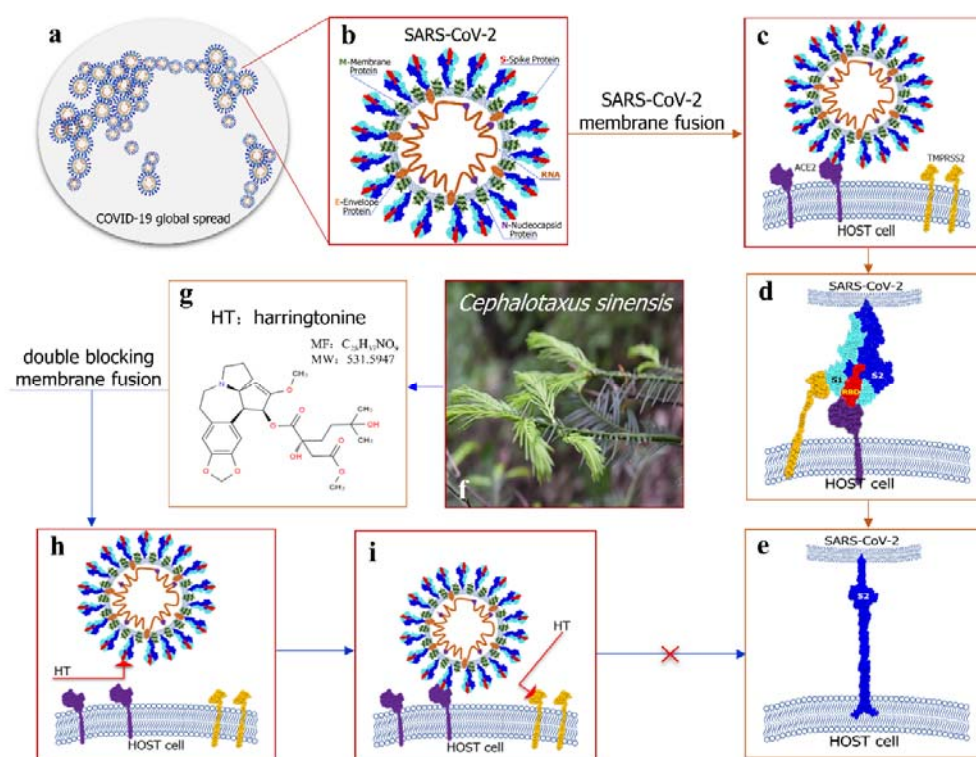


**Fig. 1 A new strategy of double blocking SARS-CoV-2 membrane fusion using harringtonine (HT).** **a**, The COVID-19 pandemic is spreading globally. **b**, SARS-CoV-2 is mainly composed of the spike (S), membrane (M), and envelope (E) proteins. There is a viral RNA chain of the nucleocapsid (N) protein inside SARS-CoV-2. **c-e**, SARS-CoV-2 membrane fusion process includes the formation of the S-ACE2 complex, which is hydrolysed by TMPRSS2 and S2 fusion peptide anchored to the host membrane. **f-g**, HT was isolated from *Cephalotaxus sinensis*. **h-i**, Our aim is to find an antagonist such as HT that blocks SARS-CoV-2 membrane fusion by simultaneously targeting S protein and the host TMPRSS2.

Natural medicinal plants are an important source of small molecule new drugs<sup>6</sup>. The *Cephalotaxus sinensis* is a unique medicinal plant from Qinling Mountains of China<sup>7</sup>, and the average content of HT is 0.0045% (**Fig 1. f-g**). In this study, we propose a new strategy of treatment to be directed against SARS-CoV-2 membrane fusion through the S protein (**Fig.1c-e**). HT, a small molecule antagonist, targets the S protein to inhibit its binding to the ACE2 receptor in host cells; simultaneously, it targets the host cell TMPRSS2 against the enzymatic hydrolysis of S protein (**Fig1. h-i**). Our experiments showed that HT is an effective antagonist and acts by double blocking SARS-CoV-2 membrane fusion.

## **1. HT Targeted the S protein of SARS-CoV-2, and to TMPRSS2 in host cells**

Cell membrane chromatography (CMC) is a biomimetic analysis technology used to study interactions between drugs and their receptors<sup>8</sup>. In this study, the S/CMC and TMPRSS2/CMC models were established to test the affinities between HT and S protein as well as TMPRSS2<sup>9</sup>. The reversibility of HT on the S protein and TMPRSS2 was determined. In addition, the binding modes of HT were simulated by computer molecular docking technology.

The  $K_D$  values of HT were  $1.36 \pm 0.10 \mu\text{M}$  (S protein) and  $15 \pm 3.34 \mu\text{M}$  (TMPRSS2)<sup>10</sup>. The  $A_S$  values were 1.71 (S protein) and 5.27(TMPRSS2) (**Fig. 2a-d**). CMD showed that HT can form hydrogen bonds with the GLY696, SER494, TYR449, and ARG403 residues in the RBD domain of the S protein (PDB ID: 6M0J), and these sites were key binding sites between the S protein and ACE2. HT can also bind the SER441, GLY462, and GLY464 residues in the domain of TMPRSS2 (PDB ID: 7MEQ) (**Fig. 2e-f**). These findings show that HT has a strong affinity for

SARS-CoV-2 S protein and TMPRSS2, and also shows some irreversibility, which is very beneficial for blocking SARS-CoV-2 membrane fusion.

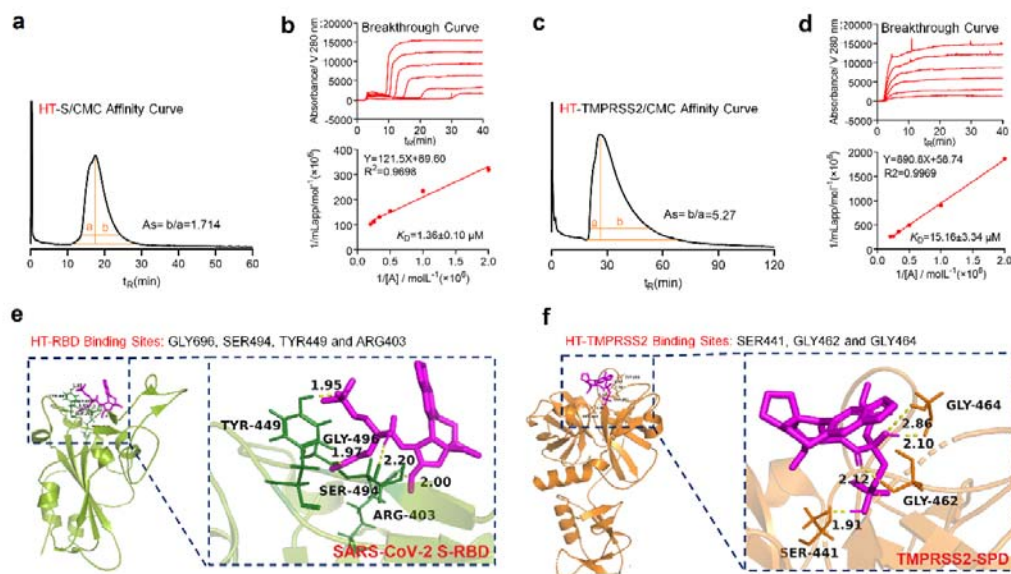


**Fig. 2** HT specifically targets the S protein of SARS-CoV-2 and host cell TMPRSS2. **a-b**, Affinity and breakthrough curves of HT were obtained using the S/CMC-HPLC method and **c-d**, the TMPRSS2/CMC-HPLC method. **e-f**, Computer molecular docking (CMD) was used to identify the hydrogen bonds between HT and the receptor-binding domain (RBD) of S protein, and those between HT and the serine protease domain (SPD) of TMPRSS2. Graphs display mean  $\pm$  S.E.M. One-way ANOVA (and nonparametric or mixed) (\* $P < 0.05$ , \*\* $P < 0.01$ , \*\*\* $P < 0.001$  vs. 0)

## 2. HT inhibits pseudotyped virus membrane fusion

The interaction between ACE2 and the S protein plays a key role in SARS-CoV-2 infection<sup>11</sup>. We used NanoBiT® to evaluate the effect of HT on the interaction between ACE2 and The S protein (**Fig. 3a**). As shown in Fig 3b, HT can dose-dependently inhibit cell-to-cell membrane fusion induced by the binding of ACE2 and S proteins (S495) (**Fig. 3b-c, and e**). In addition, HT also effectively inhibited ACE2<sup>h</sup> cell membrane fusion induced by Delta virus mutated S protein-L452R, T478K, and P681R sites (S605) (**Fig. 3b, d, and f**). It was evident from the micrographs that HT dose-dependently inhibited S495 and S605-induced syncytial formation.

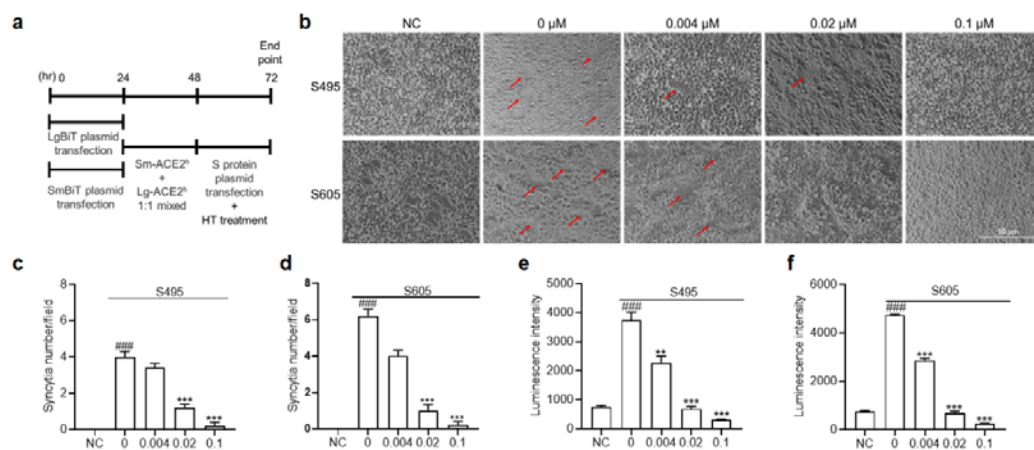


**Fig. 3 HT simultaneously membrane fusion through S protein.** **a**, Protocol of ACE2h cells membrane fusion assay; ACE2h cells were transfected with LgBit plasmid and SmBit plasmid respectively for 24h. Then, 1:1 mixed and incubated for the night. After that, mixed cells were transfected with S protein plasmid for 24h and the cells were collected and used to evaluate Luminescence intensity. **b**, HT inhibited S495 and S605 induced ACE2h cells membrane fusion. **c-d**, Quantitation of numbers of syncytia in cells as described in (b). Values are syncytia number per microscope field. **e-f**, Luciferase were measured to indicate the effect of HT to S495 and S605-induced syncytial formation. Graphs display mean  $\pm$  S.E.M. One-way ANOVA (and nonparametric or mixed) (\* $P < 0.05$ , \*\* $P < 0.01$ , \*\*\* $P < 0.001$  vs. 0)

We used a pseudotyped virus, it can be used to evaluate the antiviral effects of drugs only in a P2 Lab<sup>12,13</sup> (**Fig. 4a**). The pseudovirus has a significant infection advantage for ACE2<sup>h</sup> cells<sup>14</sup>. ACE2<sup>h</sup>/TMPRSS2<sup>h</sup> cells were successfully established by stably overexpressing TMPRSS2 in ACE2<sup>h</sup> cells<sup>15</sup>. The pseudo-type entry rates in ACE2<sup>h</sup>/TMPRSS2<sup>h</sup> cells were greatly improved compared with those in ACE2<sup>h</sup> cells when pseudotyped viruses were used to infect different cells. The ACE2<sup>h</sup>/TMPRSS2<sup>h</sup> cell model works well because the Camostat (TMPRSS2 antagonist) considered to be an effective antagonist of TMPRSS2 and can effectively inhibit pseudovirus infection (**Fig. 4b**).

The TMPRSS2 enzyme on host cells plays a key role in pseudovirus virus membrane fusion. HT dose-dependently inhibited pseudovirus infection in ACE2<sup>h</sup> and ACE2<sup>h</sup>/TMPRSS2<sup>h</sup> cells, with IC<sub>50</sub> values of  $1.091 \pm 0.157 \mu\text{M}$  and  $0.580 \pm 0.15 \mu\text{M}$ , respectively. The latter is obviously stronger than the former (**Fig. 4c-f**). The results show that HT is an effective antagonist against SARS-CoV-2 infection, and

TMPRSS2 has a key synergistic effect.

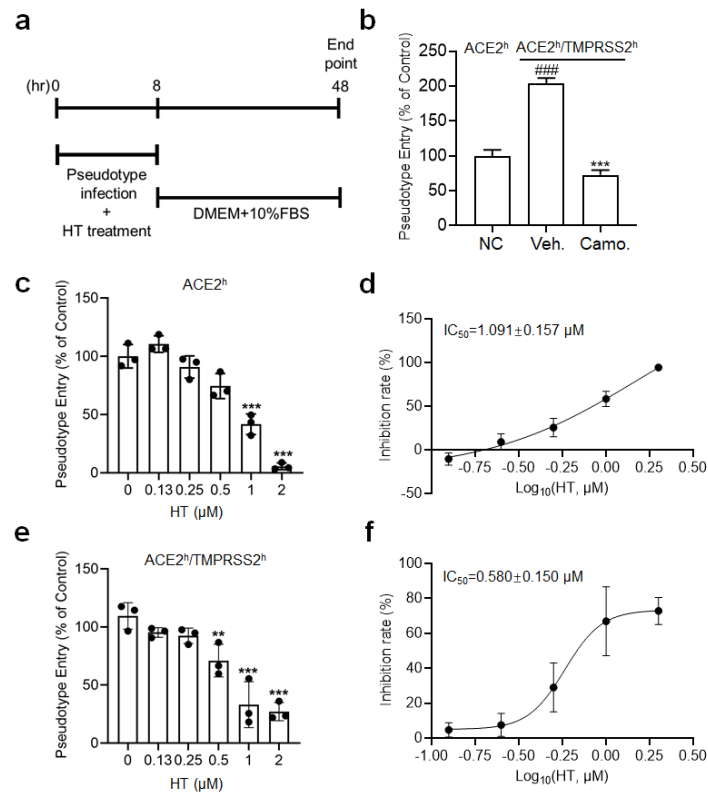


**Fig.4 Effect of HT on the entrance of SARS-CoV-2 spike pseudotyped virus into ACE2<sup>h</sup> and ACE2<sup>h</sup>/TMPRSS2<sup>h</sup> cells.** **a**, Protocol of pseudotyped virus entry assay; ACE2<sup>h</sup> cells were pretreated with pseudotyped SARS-CoV-2 virus combined with different doses of HT for 8 h. Then, the cells were transferred to fresh cell culture medium and incubated for 48 h; the cells were collected and used to evaluate pseudotype entry rates. **b**, TMPRSS2 was transfected into ACE2<sup>h</sup> cells (ACE2<sup>h</sup>/TMPRSS2<sup>h</sup> cell), which were then infected with pseudotype combined with vehicle (Veh.) or camostat (Camo.) The entrance of pseudotype virus into ACE2<sup>h</sup>/TMPRSS2<sup>h</sup> cells was inhibited by camostat. **c-d**, HT inhibited pseudotyped virus entry into ACE2<sup>h</sup> cells. **e-f**, HT inhibited pseudotyped virus entry into ACE2<sup>h</sup>/TMPRSS2<sup>h</sup> cells dose-dependently. Graphs display mean±S.E.M. One-way ANOVA (and nonparametric or mixed) (\**P*<0.05, \*\**P*<0.01, \*\*\**P*<0.001 vs. 0)

### 3. HT as an antagonist for anti-SARS-CoV-2 infection

The anti-SARS-CoV-2 effects of HT in vitro were investigated in SARS-CoV-2ΔN trVLP with N protein deficient<sup>16</sup>, SARS-CoV-2-WIV04 original strain, and SARS-CoV-2-Delta 630 mutant strain.



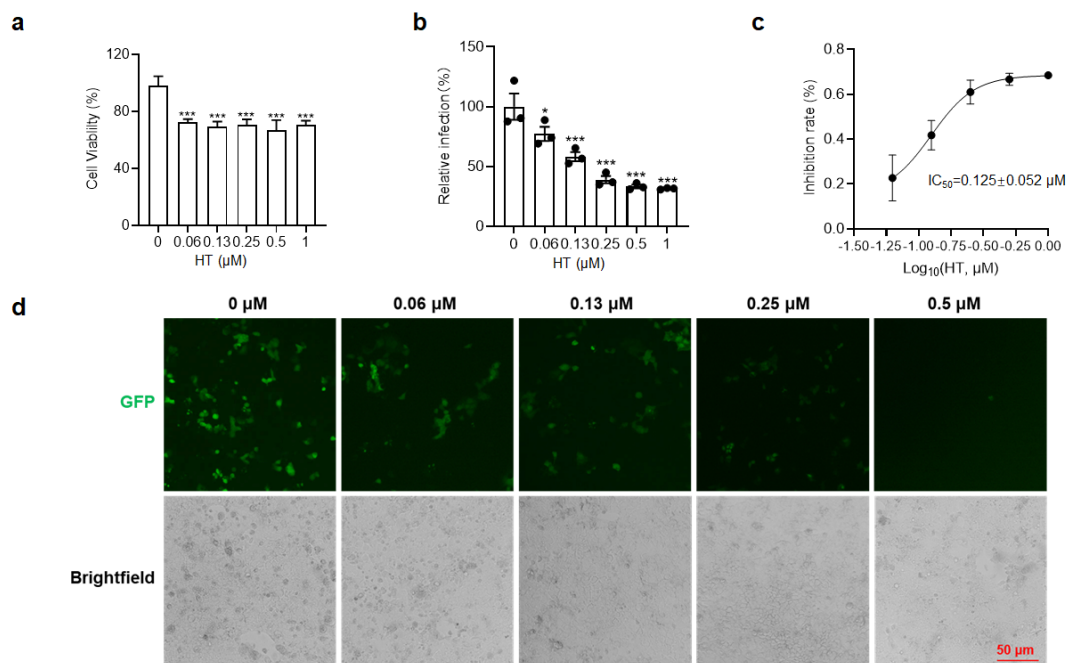


**Fig. 5 HT successfully blocks SARS-CoV-2/ΔN infecting Caco 2-N cells.** **a**, Viability of Caco2-N cells treated with 1 μM HT for 72 h. **b-c**, HT in the range of 0.06~1 μM dose-dependently decreased SARS-CoV-2ΔN trVLP infection in Caco-2-N cells. **d**, Representative image of HT inhibiting SARS-CoV-2/ΔN infecting Caco 2-N cells. Graphs display mean ± S.E.M. One-way ANOVA (and nonparametric or mixed) (\* $P < 0.05$ , \*\* $P < 0.01$ , \*\*\* $P < 0.001$  vs. 0)

The survival rate of Caco-2-N cells was more than 70% under 1 μM HT treatment (**Fig. 5a**). HT dose-dependently decreased SARS-CoV-2ΔN trVLP infection in Caco-2-N cells, with an IC<sub>50</sub> value of 0.125 ± 0.052 μM (**Fig. 5b-d**).



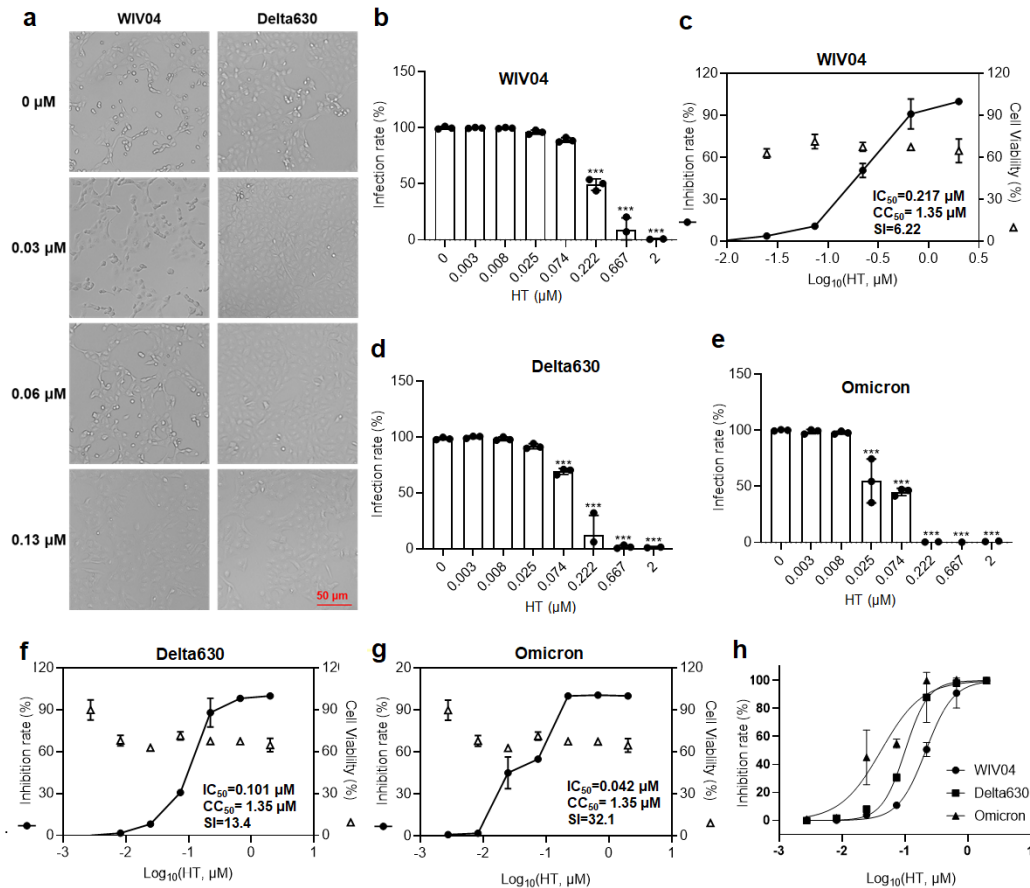


**Fig. 6 HT successfully blocks SARS-CoV-2 infection.** **a**, Representative image of HT inhibiting SARS-CoV-2-WIV04 and SARS-CoV-2-Delta 630 virus-induced cytopathic effects (CPE). **b-c**, Real-time RT-PCR showed that HT in the range of 0.03~2  $\mu\text{M}$  dose-dependently inhibited SARS-CoV-2-WIV04 virus infection in Vero E6 cells. **d-e**, Real-time RT-PCR showed that HT significantly inhibited SARS-CoV-2-Delta 630 and Omicron virus infection in Vero-E6 cells, with a lower inhibiting dose. **f-g**, The  $\text{IC}_{50}$ ,  $\text{CC}_{50}$  and SI of HT on the two variant strains of SARS-CoV-2. **h**, HT inhibits SARS-CoV-2 and its variant strains from infecting Vero E6 cells. Graphs display mean  $\pm$  S.E.M. One-way ANOVA (and nonparametric or mixed) (\* $P < 0.05$ , \*\* $P < 0.01$ , \*\*\* $P < 0.001$  vs. 0)

SARS-CoV-2-WIV04 has been one of the original strains since the outbreak of COVID-19. Vero-E6 cells are African green monkey kidney cell lines that highly express the ACE2 receptor<sup>17</sup>. In Vero E6, HT dose-dependently inhibited the cytopathic effect CPE caused by WIV04 virus (**Fig. 6a**). In Vero E6 cells, the  $\text{CC}_{50}$  and  $\text{IC}_{50}$  values of HT were 1.35  $\mu\text{M}$  and 0.217  $\mu\text{M}$ , respectively, and the selectivity index ( $\text{SI} = \text{CC}_{50}/\text{EC}_{50}$ ) was 6.22 (**Fig. 6b-c**). Repeated epidemics are caused by the constant mutation of the SARS-CoV-2. The delta mutant strain was found in India as

early as October 2020<sup>18,19</sup> rapidly spreading and became a major concern in the containment of the pandemic<sup>20,21</sup>. On November 9, 2021, the first Omicron sequence available was from a specimen collected in Botswana. Ever since the identification of Omicron, the variant appears to rapidly spread. At the time of this writing, Omicron has become a major concern in the containment of the current pandemic<sup>22,23</sup>. The same evaluation tests for HT were performed on the Delta 630 and Omicron mutant. The results further confirmed that HT inhibit SARS-CoV-2-Delta 630 virus and Omicron infections at a lower inhibitory dose of 0.074  $\mu\text{M}$  and 0.025  $\mu\text{M}$  (**Fig. 6d-e**). The  $\text{IC}_{50}$  value of HT was as low as 0.101  $\mu\text{M}$  and 0.042  $\mu\text{M}$ , with a SI value of 13.4 and 32.1, which was almost five times that of the WIV04 original strain (**Fig. 6f-g**). With the increase of mutation sites on RBD, the antiviral effect of HT was significantly enhanced rather than decreased (**Fig. 6h**).

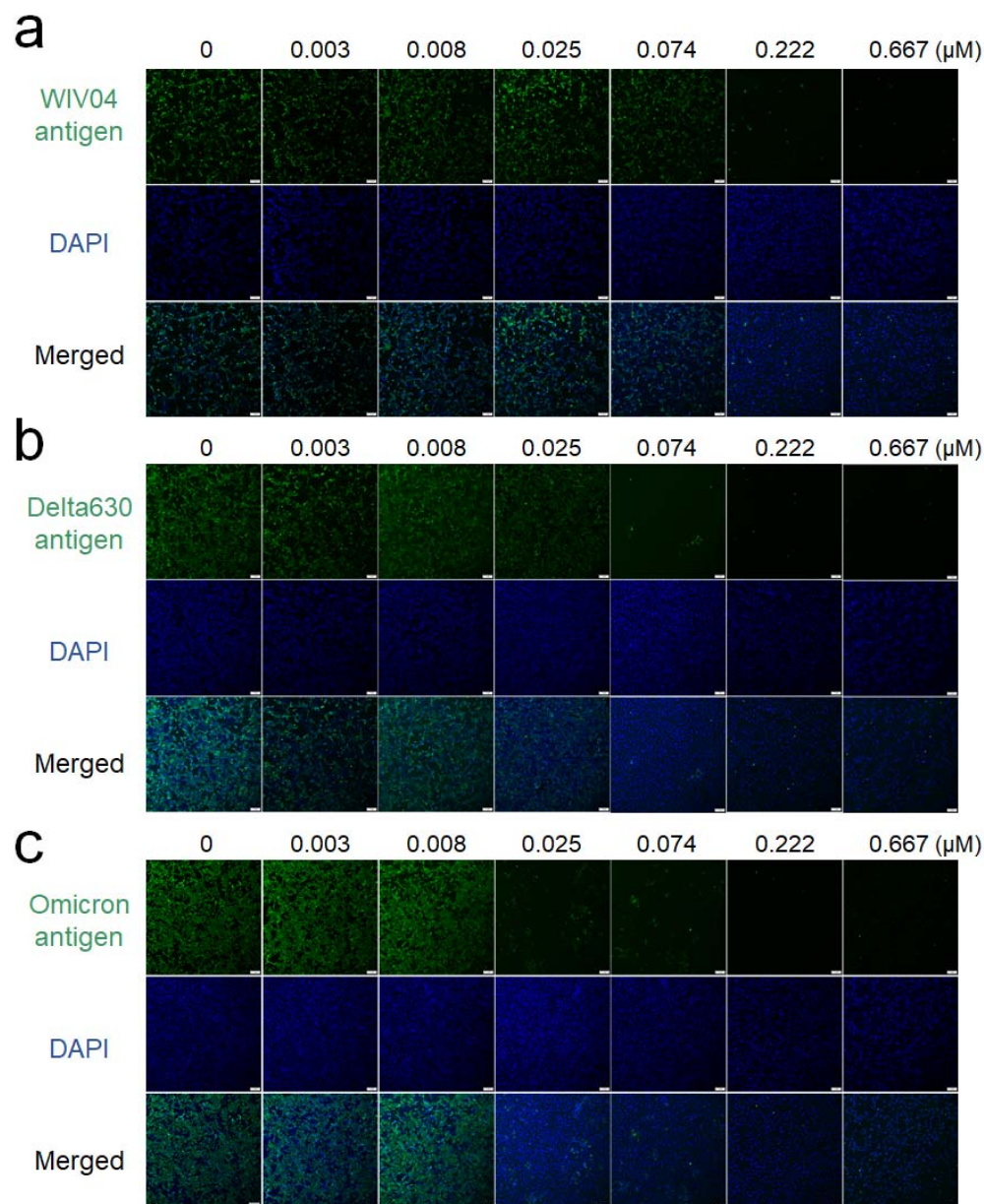


**Fig.7 Representative immunofluorescence images of HT significantly inhibited SARS-CoV-2 infection.** **a**, Immunofluorescence showed that HT significantly inhibited SARS-CoV-2-WIV04 virus infection in Vero-E6 cells. **b**, Immunofluorescence showed that HT significantly inhibited SARS-CoV-2-Delta 630 virus infection in Vero-E6 cells. **c**, Immunofluorescence showed that HT significantly inhibited SARS-CoV-2-Omicron virus infection in Vero-E6 cells, with a lower inhibiting dose. The scale of the figure is 1 mm.

In line with the viral immunofluorescence, the expression of S protein was dramatically decreased in those cells treated with 0.222  $\mu\text{M}$  (**Fig.7a**); for Delta630, 0.074  $\mu\text{M}$  treatment could result in significantly less S protein expression compared to

the untreated infected cells (**Fig.7b**); for Omicron, even 0.025  $\mu\text{M}$  treatment could result in significantly less S protein expression compared to the untreated infected cells (Fig.7c). Thus, these findings show that HT is exceptionally valuable for anti-SARS-CoV-2 therapy. In summary, this study confirms that HT can inhibit SARS-CoV-2 membrane fusion by double blocking the S protein and TMPRSS2 pathway, thereby making it an effective antagonist for SARS-CoV-2 infection.

## **Conclusion**

Collectively, HT has two potential advantages in the clinical treatment of COVID-19. First, HT mainly targets the S protein and inhibits its ability to bind to ACE2 protein on host cells. Compared with anti-SARS-CoV-2 replication drugs, HT greatly reduces the damage of S protein's autotoxicity to the organ system. Second, with continuing variation of SARS-CoV-2, the virus will "escape" the recognition of neutralizing antibodies and antibodies produced by inactivated vaccines. However, HT, as a small molecule antagonist, is minimally affected by SARS-CoV-2 variation. At present, the increased infectivity of Omicron reflects that it is stronger membrane fusion effect<sup>24</sup>. TH, as a small molecule antagonist for membrane fusion, is more targeted and can effectively block Omicron infection.

## **Conflicts of Interest**

The authors declare no competing financial interest.

## **Acknowledgement**

This work was cofounded by National Natural Science Foundation of China (Grant number: 82150201 and 81930096) and the Major Research Development Program of Shaanxi Province (Grant number: 2022ZDXM-SF-03) .

## References

- 1 Yu, S. *et al.* Comparison and Analysis of Neutralizing Antibody Levels in Serum after Inoculating with SARS-CoV-2, MERS-CoV, or SARS-CoV Vaccines in Humans. *Vaccines (Basel)* **9**, doi:10.3390/vaccines9060588 (2021).
- 2 Aziz, F., Bath, J. & Smeds, M. R. Implications of the severe acute respiratory syndrome associated with the novel coronavirus-2 on vascular surgery practices. *J Vasc Surg* **73**, 4-11 e12, doi:10.1016/j.jvs.2020.08.118 (2021).
- 3 Singhal, T. A Review of Coronavirus Disease-2019 (COVID-19). *Indian J Pediatr* **87**, 281-286, doi:10.1007/s12098-020-03263-6 (2020).
- 4 Dyer, O. Covid-19: South Africa's surge in cases deepens alarm over omicron variant. *BMJ* **375**, n3013, doi:10.1136/bmj.n3013 (2021).
- 5 Planas, D. *et al.* Reduced sensitivity of SARS-CoV-2 variant Delta to antibody neutralization. *Nature* **596**, 276+ (2021).
- 6 Chen, R. R., Li, Y. J., Chen, J. J. & Lu, C. L. A review for natural polysaccharides with anti-pulmonary fibrosis properties, which may benefit to patients infected by 2019-nCoV. *Carbohydr Polym* **247**, 116740, doi:10.1016/j.carbpol.2020.116740 (2020).
- 7 Powell, R. G., Weisleder, D., Smith, C. R., Jr. & Rohwedder, W. K. Structures of harringtonine, isoharringtonine, and homoharringtonine. *Tetrahedron Lett*, 815-818, doi:10.1016/s0040-4039(01)97839-6 (1970).
- 8 Ma, W. *et al.* Advances in cell membrane chromatography. *J Chromatogr A* **1639**,

- 461916, doi:10.1016/j.chroma.2021.461916 (2021).
- 9 Fu, J. *et al.* Targeting and Covalently Immobilizing the EGFR through SNAP-Tag Technology for Screening Drug Leads. *Anal Chem* **93**, 11719-11728, doi:10.1021/acs.analchem.1c01664 (2021).
- 10 Ma, W., Yang, L. & He, L. Overview of the detection methods for equilibrium dissociation constant  $K_D$  of drug-receptor interaction. *J Pharm Anal* **8**, 147-152, doi:10.1016/j.jpha.2018.05.001 (2018).
- 11 Hoffmann, M. *et al.* SARS-CoV-2 Cell Entry Depends on ACE2 and TMPRSS2 and Is Blocked by a Clinically Proven Protease Inhibitor. *Cell* **181**, 271-280 e278, doi:10.1016/j.cell.2020.02.052 (2020).
- 12 Johnson, M. C. *et al.* Optimized Pseudotyping Conditions for the SARS-COV-2 Spike Glycoprotein. *J Virol* **94**, doi:10.1128/JVI.01062-20 (2020).
- 13 Ou, X. *et al.* Characterization of spike glycoprotein of SARS-CoV-2 on virus entry and its immune cross-reactivity with SARS-CoV. *Nat Commun* **11**, 1620, doi:10.1038/s41467-020-15562-9 (2020).
- 14 Kim, T. Y. *et al.* Platycodin D, a natural component of *Platycodon grandiflorum*, prevents both lysosome- and TMPRSS2-driven SARS-CoV-2 infection by hindering membrane fusion. *Exp Mol Med* **53**, 956-972, doi:10.1038/s12276-021-00624-9 (2021).
- 15 Li, K., Meyerholz, D. K., Bartlett, J. A. & McCray, P. B., Jr. The TMPRSS2 Inhibitor Nafamostat Reduces SARS-CoV-2 Pulmonary Infection in Mouse Models of COVID-19. *mBio* **12**, e0097021, doi:10.1128/mBio.00970-21 (2021).



- 16 Ju, X. *et al.* A novel cell culture system modeling the SARS-CoV-2 life cycle. *PLoS Pathog* **17**, e1009439, doi:10.1371/journal.ppat.1009439 (2021).
- 17 Li, W. H. *et al.* Angiotensin-converting enzyme 2 is a functional receptor for the SARS coronavirus. *Nature* **426**, 450-454, doi:10.1038/nature02145 (2003).
- 18 Brown, C. M. *et al.* Outbreak of SARS-CoV-2 Infections, Including COVID-19 Vaccine Breakthrough Infections, Associated with Large Public Gatherings - Barnstable County, Massachusetts, July 2021. *MMWR Morb Mortal Wkly Rep* **70**, 1059-1062, doi:10.15585/mmwr.mm7031e2 (2021).
- 19 Dougherty, K., Mannell, M., Naqvi, O., Matson, D. & Stone, J. SARS-CoV-2 B.1.617.2 (Delta) Variant COVID-19 Outbreak Associated with a Gymnastics Facility - Oklahoma, April-May 2021. *MMWR Morb Mortal Wkly Rep* **70**, 1004-1007, doi:10.15585/mmwr.mm7028e2 (2021).
- 20 Barua, S. *et al.* Identification of the SARS-CoV-2 Delta variant C22995A using a high-resolution melting curve RT-FRET-PCR. *Emerg Microbes Infect*, 1-11, doi:10.1080/22221751.2021.2007738 (2021).
- 21 Shrestha, L. B., Tedla, N. & Bull, R. A. Broadly-Neutralizing Antibodies Against Emerging SARS-CoV-2 Variants. *Front Immunol* **12**, 752003, doi:10.3389/fimmu.2021.752003 (2021).
- 22 He, X., Hong, W., Pan, X., Lu, G. & Wei, X. SARS-CoV-2 Omicron variant: Characteristics and prevention. *MedComm (2020)*, doi:10.1002/mco2.110 (2021).
- 23 Cameroni, E. *et al.* Broadly neutralizing antibodies overcome SARS-CoV-2 Omicron antigenic shift. *Nature*, doi:10.1038/s41586-021-04386-2 (2021).

- 24 VanBlargan, L. A. *et al.* An infectious SARS-CoV-2 B.1.1.529 Omicron virus escapes neutralization by therapeutic monoclonal antibodies. *Nat Med*, doi:10.1038/s41591-021-01678-y (2022).